MULTISTRANGE HYPERON PRODUCTION ON NUCLEAR TARGETS*

C. Merino

Departamento de Física de Partículas, Facultade de Física
Instituto Galego de Física de Altas Enerxías
(María de Maeztu Unit of Excellence)
Universidade de Santiago de Compostela
Galiza, Spain
carlos.merino@usc.gal

*Received 14 December 2024, accepted 10 January 2025,
published online 6 March 2025*

The study of the production of strange Λs and multistrange baryons (Ξ, Ω) and antibaryons on nuclear targets at the energy region from SPS up to LHC in the framework of the Quark–Gluon String Model is presented and compared with the available experimental data. The most significant results of this analysis is the significant dependence on the centrality of the collision of the experimental $\bar{\Xi}^+/\bar{\Lambda}$ and $\bar{\Omega}^+/\bar{\Lambda}$ ratios in heavy-ion collisions, at SPS energies.

DOI:10.5506/APhysPolBSupp.18.1-A2

1. Production of strangeness in the QGSM

The predictions and results obtained in the framework of the Quark–Gluon String Model (QGSM) are presented and compared [1–4] with the experimental data on yields of Λ, Ξ, and Ω baryons and the corresponding antibaryons in nucleus–nucleus collisions for a wide energy region going from SPS up to LHC. We also consider the ratios of multistrange to strange antihyperon production in nucleus–nucleus collisions with different centralities in the same energy range.

The QGSM [5] is based on the Dual Topological Unitarization, Regge phenomenology, and nonperturbative notions of QCD. In QGSM, high-energy interactions are considered as proceeding via the exchange of one or several Pomerons. The cut of at least some of those Pomerons determines the inelastic scattering amplitude of the particle production processes. In the case of interaction with a nuclear target, the Multiple Scattering Theory

* Presented at the Diffraction and Low-x 2024 Workshop, Trabia, Palermo, Italy, 8–14 September, 2024.

(Gribov–Glauber Theory) is used. At very high energies, the contribution of enhanced Reggeon diagrams leads to the suppression of the inclusive density of secondaries into the central (midrapidity) region. The QGSM provides a successful description of multiparticle production in hadron–hadron, hadron–nucleus, and nucleus–nucleus collisions for a wide energy region.

The QGSM [6] provides quantitative predictions of different features of multiparticle production, in particular, of the inclusive densities of different secondaries, both in the central and in the beam fragmentation regions. In QGSM, high-energy hadron–nucleon collisions are implemented through the exchange of one or several Pomerons, all elastic and inelastic processes resulting from cutting between (elastic) or through (inelastic) Pomerons [7].

It was assumed in the QGSM that the Pomeron corresponding to the cylinder-type diagrams is a simple pole with $\alpha_P(0) > 1$ (supercritical Pomeron).

The inclusive spectrum of a secondary hadron h is then determined by the convolution of the diquark, valence quark, and sea quark distribution functions, $u(x,n)$ (every one normalized to unity), in the incident particles with the fragmentation functions $G^h(z)$ for quarks and diquarks to contribute to the production of the secondary hadron h. Both the distribution functions and the fragmentation functions are constructed by using the well-established Reggeon counting rules. The average number of exchanged Pomerons slowly increases with the energy of the collision.

The production of multistrange hyperons, Ξ^- (dss) and Ω^- (sss), has special interest in high-energy particle and nuclear physics. The production of each additional strange quark featuring in the secondary baryons, *i.e.* the production rate of secondary $B(qqs)$ over secondary $B(qqq)$, then of $B(qss)$ over $B(qqs)$, and, finally, of $B(sss)$ over $B(qss)$, is affected by one universal strangeness suppression factor, λ_{s},

$$\lambda_{\mathrm{s}} = \frac{B(qqs)}{B(qqq)} = \frac{B(qss)}{B(qqs)} = \frac{B(sss)}{B(qss)} \tag{1}$$

together with some simple quark combinatorics.

Let us define

$$R\left(\bar{\Xi}^+/\bar{\Lambda}\right) = \frac{\mathrm{d}n}{\mathrm{d}y}\left(A+B \to \bar{\Xi}^+ + X\right) \Big/ \frac{\mathrm{d}n}{\mathrm{d}y}\left(A+B \to \bar{\Lambda} + X\right) , \tag{2}$$

$$R\left(\bar{\Omega}^+/\bar{\Lambda}\right) = \frac{\mathrm{d}n}{\mathrm{d}y}\left(A+B \to \bar{\Omega}^+ + X\right) \Big/ \frac{\mathrm{d}n}{\mathrm{d}y}\left(A+B \to \bar{\Lambda} + X\right) . \tag{3}$$

The ratios in Eqs. (2) and (3) can be calculated in the QGSM as a function of the strangeness suppression parameter, λ_{s}, and the corresponding QGSM results reasonably describe the experimental data for a large energy range, when a relatively small number of incident nucleons participate in the collision (nucleon–nucleus collisions, or peripheral nucleus–nucleus collisions), by thoroughly using the value $\lambda_s = 0.32$ to fit those experimental values. The ratio of yields of different particles should not depend, in principle, on the centrality of the collision [1].

2. Centrality dependence of antihyperon production in heavy-ion collisions

In Fig. 1, we show the comparison of the QGSM prediction with the experimental data [8] on the dependence of the ratios $\bar{\Omega}^+/\bar{\Lambda}$ (left panel) and $\bar{\Xi}^+/\bar{\Lambda}$ (right panel) on the number of wounded nucleons, N_w, in Pb+Pb collisions at 158 GeV/c per nucleon. Small values of N_w correspond to peripheral collisions (large impact parameter), while large values of N_w corresponds to central collisions (small impact parameter).

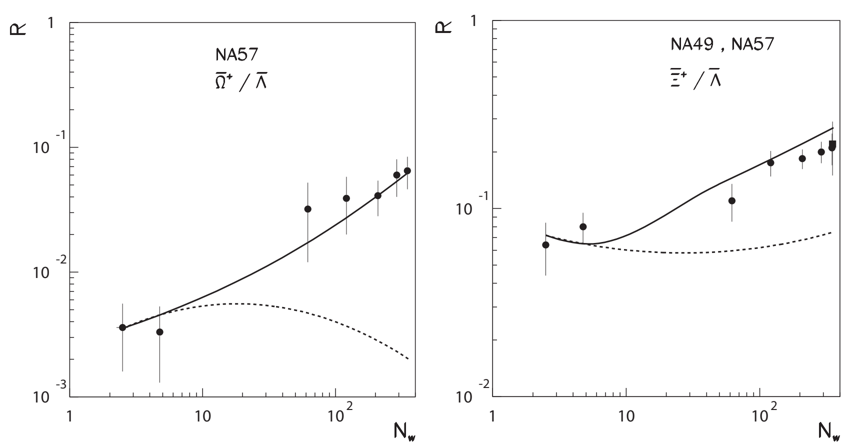

Fig. 1. Experimental SPS ratios $\bar{\Omega}^+/\bar{\Lambda}$ (left panel) and of $\bar{\Xi}^+/\bar{\Lambda}$ (right panel) in Pb+Pb collisions as a function of the number of wounded nucleons, N_w, compared with the corresponding QGSM results. The full lines show the result of the QGSM calculation obtained with the value $\lambda_s = 0.32$ at the left end and with larger values of λ_s at its right end, while the dashed lines show the result of the QGSM calculation obtained with a constant value $\lambda_s = 0.32$, disregarding of the value of the number of wounded nucleons (centrality).

At small values of N_w, the ratio is practically equal to that in the cases of p+Be and p+Pb collisions, and they all can be correctly described by the QGSM by using a value of the strangeness suppression parameter, $\lambda_s = 0.32$. However, the experimental ratio increases rather fast with the increasing value of N_w, *i.e.* when we move from peripheral to central Pb+Pb collisions, being central heavy-nuclei collisions the first case in which a different (larger than $\lambda_s = 0.32$) value of the strangeness suppression parameter is needed to fit the result of the QGSM calculation to the experimental data on the ratios $R(\bar{\Xi}^+/\bar{\Lambda})$ and $R(\bar{\Omega}^+/\bar{\Lambda})$. This unexpected behaviour in the case of central heavy-nuclei collisions is shown by the full line in Fig. 1, that has been calculated with the value $\lambda_s = 0.32$ at its left end and with larger values of λ_s at its right end (see Ref. [1] for details). The results of QGSM calculations with a constant value $\lambda_s = 0.32$, disregarding of the value of the number of wounded nucleons (centrality), N_w, are shown in Fig. 1 by dashed lines.

This behaviour in which the value of the strangeness suppression factor λ_s increases with the value of N_w (centrality), indicates (see [1] for details) that the simple quark combinatorial rules are not valid for central collisions of heavy nuclei.

Now, we consider the experimental data on midrapidity densities of hyperons in Au+Au collisions measured by the STAR Collaboration [9–11] at RHIC energies.

In Fig. 2, we present the comparison of the QGSM predictions with experimental data on the N_w dependence of the ratios $\bar{\Omega}^+/\bar{\Lambda}$ (left panel) and $\bar{\Xi}^+/\bar{\Lambda}$ (right panel), measured by the STAR Collaboration in the midrapidity region at $\sqrt{s} = 62.4$ GeV. Similarly as in Fig. 1, the left end of the full line here was calculated with a value $\lambda_s = 0.32$, while for the right end larger

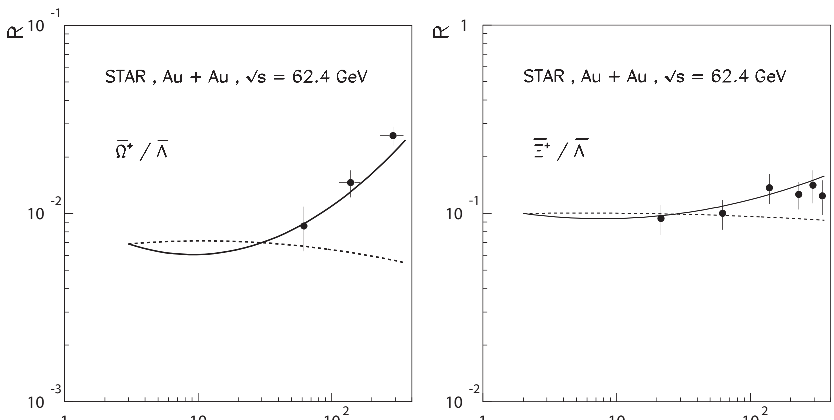

Fig. 2. Experimental STAR Collaboration ratios $\bar{\Omega}^+/\bar{\Lambda}$ (left panel) and $\bar{\Xi}^+/\bar{\Lambda}$ (right panel) in Au+Au collisions at $\sqrt{s} = 62.4$ GeV as a function of the number of wounded nucleons, N_w, compared with the corresponding QGSM results. The full lines show the result of the QGSM calculation obtained with the value $\lambda_s = 0.32$ at the left end and with larger values of λ_s at its right end, while the dashed lines show the result of the QGSM calculation obtained with a constant value $\lambda_s = 0.32$, disregarding of the value of the number of wounded nucleons (centrality).

values of λ_s were used [1]. The dashed line was calculated with a constant value of $\lambda_s = 0.32$. We see here that the value of λ_s that correctly describes multistrange hyperon production at RHIC energies is larger than the one for the case of Λ and $\bar{\Lambda}$ production, though the difference between those two values of λ_s is not so large as it is for collisions at lower energies. This seems to indicate that the difference in the values of the parameter λ_s, for multistrange hyperon, and for Λ and $\bar{\Lambda}$ production, decreases with the growing of the initial energy of the collision.

In Table 1, we consider the experimental data on Ξ^-, $\bar{\Xi}^+$, Ω^-, $\bar{\Omega}^+$ production in central Pb+Pb collisions at $\sqrt{s} = 2.76$ TeV measured by the ALICE Collaboration [12] at the CERN LHC. Now, the strangeness suppression parameter λ_s for Ξ^- and $\bar{\Xi}^+$ production becomes smaller than at RHIC energies, taking the standard value $\lambda_s = 0.32$. In the case of Ω^- and $\bar{\Omega}^+$ production, the value of λ_s also decreases with respect to the RHIC energy range. Thus, we see that the unusually large values of λ_s for central Pb+Pb collisions at 158 GeV/c per nucleon, monotonically decrease with the increase of the initial energy of the collision.

Table 1. Experimental data on dn/dy of Ξ^- and of Ξ^-, $\bar{\Xi}^+$, Ω^-, and $\bar{\Omega}^+$ production in central Pb+Pb collisions at $\sqrt{s} = 2.76$ TeV per nucleon by the ALICE Collaboration [12], compared with the corresponding QGSM results.

Process	$\sqrt{s}$ [TeV]	Centrality	dn/dy (experimental data)	dn/dy (QGSM)	λ_s
Pb+Pb$\to \Xi^-$	2.76	0–10%	$3.34 \pm 0.06 \pm 0.24$	3.357	0.32
Pb+Pb $\to \bar{\Xi}^+$	2.76	0–10%	$3.28 \pm 0.06 \pm 0.23$	3.317	
Pb+Pb $\to \Omega^-$	2.76	0–10%	$0.58 \pm 0.04 \pm 0.09$	0.606	0.38
Pb+Pb $\to \bar{\Omega}^+$	2.76	0–10%	$0.60 \pm 0.05 \pm 0.09$	0.601	

3. Conclusion

The experimental data on the production of hyperons in central collisions of heavy nuclei present a very significant centrality dependence at CERN-SPS energies $\sqrt{s} = 17.3$ GeV. This dependence decreases when the initial energy of the collision grows, *i.e.* at RHIC and LHC energies. No consistent theoretical explanation of this unexpected experimental fact is currently known, but some intrinsic dynamical difference between the central and the peripheral interactions must be responsible for it. We intend to investigate further the dynamics behind this specific behaviour of the central heavy-nuclei collisions, and we would like also to draw the attention of the experimental collaborations to this point.

I want to express my deep gratitude to Gevorg H. Arakelyan and Yuli M. Shabelski, coauthors of the work on which this paper is based. It is also a pleasure to congratulate Professor Alessandro Papa and all the members of the organization of Diffraction and Low-x 2024 for a great meeting, and to thank them for their help.

REFERENCES

[1] G.H. Arakelyan, C. Merino, Yu.M. Shabelski, *Phys. Rev. D* **105**, 114013 (2022), arXiv:2112.01096 [hep-ph].

[2] G.H. Arakelyan, C. Merino, Yu.M. Shabelski, *EPJ Web Conf.* **271**, 08007 (2022), arXiv:2209.14680 [hep-ph].

[3] G.H. Arakelyan, C. Merino, Yu.M. Shabelski, *PoS* **(ICHEP2022)**, 441 (2022).

[4] G.H. Arakelyan, C. Merino, Yu.M. Shabelski, *SciPost Phys. Proc.* **15**, 024 (2024).

[5] A.B. Kaidalov, K.A. Ter-Martirosian, *Phys. Lett. B* **117**, 247 (1982).

[6] A.B. Kaidalov, K.A. Ter-Martirosyan, *Sov. J. Nucl. Phys.* **39**, 979 (1984) [*Yad. Fiz.* **39**, 1545 (1984)]; *Sov. J. Nucl. Phys.* **40**, 135 (1984) [*Yad. Fiz.* **40**, 211 (1984).

[7] V.A. Abramovsky, V.N. Gribov, O.V. Kancheli, *Sov. J. Nucl. Phys.* **18**, 308 (1973) [*Yad. Fiz.* **18**, 595 (1973)].

[8] NA57 Collaboration (F. Antinori *et al.*), *J. Phys. G: Nucl. Part. Phys.* **32**, 427 (2006), arXiv:nucl-ex/0601021.

[9] STAR Collaboration (J. Adams *et al.*), *Phys. Rev. Lett.* **92**, 182301 (2004), arXiv:nucl-ex/0307024.

[10] STAR Collaboration (J. Adams *et al.*), *Phys. Rev. Lett.* **98**, 062301 (2007), arXiv:nucl-ex/0606014.

[11] STAR Collaboration (M.M. Aggarwal *et al.*), *Phys. Rev. C* **83**, 024901 (2011), arXiv:1010.0142 [nucl-ex].

[12] ALICE Collaboration (B. Abelev *et al.*), *Phys. Lett. B* **728**, 216 (2014), *Erratum ibid.* **734**, 409 (2014), arXiv:1307.5543 [nucl-ex].